SYNTHESIS, CHARACTERIZATION AND EVALUATION OF THE PHOTOCATALYTIC ACTIVITY OF COPPER-DOPED TITANIUM DIOXIDE NANOPARTICLES IN THE DEGRADATION OF ACETOMINOPHEN

Y. Franco[a]*, J. Castillo[b] y J.C. Pereira[a]

[a] Laboratorio de Petróleo, Hidrocarburos y Derivados (PHD). Departamento de Química, Universidad de Carabobo. Venezuela.
[b] Laboratorio de Espectroscopía Láser y Nanotecnología. Escuela de Química, Universidad Central de Venezuela. Venezuela.

*yhosmaryfranco@gmail.com, +584140409491.

Received: 15-07-2024 Accepted: 12-09-2024
Published: 27-03-2025

ABSTRACT
In photocatalytic reactions, titanium dioxide (TiO_2) has been widely used as a photocatalyst for air and water decontamination, proving to be highly effective over the years. However, its activation capacity with visible light is limited by the high bandgap value of this compound. To overcome this limitation, various modifications have been implemented, such as metal doping. The aim of this study was to synthesize, characterize and evaluate the photocatalytic activity of copper-doped titanium dioxide nanoparticles (NPs) in the degradation of acetaminophen (ACF), an emerging contaminant of pharmaceutical origin. For the synthesis of Cu/TiO_2 NPs, mechanical milling and wet impregnation techniques with copper sulfate pentahydrate as a precursor were used. The characterization was carried out using various techniques, such as dynamic light scattering (DLS), scanning electron microscopy (SEM), energy dispersive X-ray spectroscopy (EDS), atomic force microscopy (AFM) and ultraviolet-visible spectroscopy (UV-Vis). The results obtained reveal a reduction of the bandgap in the Cu/TiO_2 sample, indicating a higher efficiency in the absorption of visible light. In the photocatalytic evaluation, a significant improvement in the degradation of acetaminophen (77%) was observed when using copper-doped titanium dioxide nanoparticles. These findings suggest a great potential in the application of Cu-doped TiO_2 NPs for the decontamination of waters with the presence of emerging contaminants.

Keywords: photocatalysis; nanoparticles; titanium dioxide; copper; acetaminophen.

Síntesis, caracterización y evaluación de la actividad fotocatalítica de nanopartículas de dióxido de titanio dopado con cobre en la degradación de acetaminofén

RESUMEN
En las reacciones fotocatalíticas, el dióxido de titanio (TiO_2) ha sido ampliamente utilizado como fotocatalizador para la descontaminación de aire y aguas, demostrando ser altamente efectivo a lo largo de los años. Sin embargo, su capacidad de activación con luz visible se ve limitada por el alto valor del bandgap de este compuesto. Para superar esta limitación, se han implementado diversas modificaciones, como el dopaje con metales. El objetivo de este estudio fue sintetizar, caracterizar y evaluar la actividad fotocatalítica de nanopartículas (NP) de dióxido de titanio dopado con cobre en la degradación de acetaminofén (ACF), un contaminante emergente de origen farmacéutico. Para la síntesis de las NP Cu/TiO_2 se emplearon técnicas de molienda mecánica e impregnación húmeda con sulfato de cobre pentahidratado como precursor. La caracterización se llevó a cabo mediante diversas técnicas, como dispersión dinámica de luz (DLS), microscopía electrónica de barrido (MEB), espectroscopía de rayos X de energía dispersiva (EDX), microscopía de fuerza atómica (AFM) y espectroscopía ultravioleta-visible (UV-Vis). Los resultados obtenidos revelan una reducción del bandgap en la muestra de Cu/TiO_2, lo que indica una mayor eficiencia en la absorción de luz visible. En la evaluación fotocatalítica, se observó una significativa mejora en la degradación del acetaminofén (77%) al utilizar las nanopartículas de dióxido de titanio dopadas con cobre. Estos hallazgos sugieren un gran potencial en la aplicación de las NP TiO_2 dopadas con Cu para la descontaminación de aguas con presencia de contaminantes emergentes.

Palabras claves: fotocatálisis, nanopartículas, dióxido de titanio, cobre, acetaminofén.

INTRODUCTION

More than 80% of wastewater resulting from human activity is dumped into rivers or the sea without any treatment, which causes the contamination of different bodies of water, both surface and underground, with a wide variety of substances that They can affect both ecosystems and people. In recent years, special attention has been paid to new types of contaminants present in water, such as pharmaceuticals and personal care products, as well as a variety of compounds that act as endocrine disruptors and potentiators of adverse effects on human health. and the environment. This new category of water pollutants is known as *emerging pollutants* (EC) [1, 2].

Within the list of emerging substances of pharmaceutical origin registered by the Norman Network database, is acetaminophen (NS00000231) [3]. As an emerging contaminant, acetaminophen can affect different trophic levels in an irreversible and persistent manner [4]. Over the past few years, an increase in the concentration of acetaminophen has been observed in aquatic environments, indicating that it is not completely removed from wastewater during treatment at plants, nor during infiltration into groundwater. Therefore, most acetaminophen reaches and leaks into the aquatic environment, groundwater, and drinking water through wastewater discharges [5].

The incomplete degradation of emerging contaminants in water treatment plants, added to the lack of specialized treatment in sources such as hospitals and industries, make it necessary to implement alternative and/or additional, specialized and efficient processes to carry out adequate degradation and mineralization of these pollutants [6, 7].

Water treatments by advanced oxidation processes (AOPs) constitute an alternative of great interest to address the problem of emerging contaminants, promoting their degradation to simpler substances that are harmless. OAPs are methods of treating substrates by oxidation, with radicals produced from chemical reactions. Heterogeneous photocatalysis is an advanced oxidation process that uses the photochemical method to produce the degradation of organic molecules by breaking structural bonds of contaminating organic compounds. This process uses light as the only source of energy, does not require the addition of chemical species, and its reactors are reusable and can operate in continuous processes, which further contributes to reducing costs [8].

The heterogeneous photocatalytic process is based on the excitation of a solid, commonly a wide energy gap semiconductor such as TiO_2, by irradiating it with light of an energy equal to or greater than its bandgap. This causes the transition of an electron from the valence band (VB) to the conduction band (CB), thus generating reactive species photogenerated electron-hole pairs (e^-/h^+) (Equation 1). Holes (h^+) can be trapped by water molecules (H_2O) or hydroxyl groups (^-OH) adsorbed on the surface, producing hydroxyl radicals (HO•) (Equations 2 and 3), which have a high oxidative potential (approx. 1.7 mV) and are highly reactive with organic matter, being equally toxic for microorganisms (Equations 10 and 11) [9]. Likewise, the oxygen present in the air can act as a receptor for photogenerated electrons (e^-), reacting with them to form superoxide radical anions ($•O^{2-}$), which in turn react with water to produce hydroxyl radicals (Equations 4 and 5). This process triggers a series of reactions that contribute to the photocatalytic degradation of organic contaminants (Equations 6 – 9) [10].

$$TiO_2 + hv \rightarrow TiO_2\,(e_{cb}^- + h_{vb}^+) \quad \text{(Eq. 1)}$$

$$h_{vb}^+ + H_2O \rightarrow H^+ + \bullet OH \quad \text{(Eq. 2)}$$

$$h_{vb}^+ + {}^-OH \rightarrow \bullet OH \quad \text{(Eq. 3)}$$

$$e_{cb}^- + O_2 \rightarrow \bullet O_2^- \quad \text{(Eq. 4)}$$

$$\bullet O_2^- + H_2O \rightarrow HO_2\bullet + \bullet OH \quad \text{(Eq. 5)}$$

$$HO_2\bullet + H_2O \rightarrow H_2O_2 + \bullet OH \quad \text{(Eq. 6)}$$

$$e_{cb}^- + H_2O_2 \rightarrow \bullet OH + HO^- \quad \text{(Eq. 7)}$$

$H_2O_2 + hv \rightarrow 2OH \bullet$ (Eq. 8)

$H_2O_2 + \bullet O_2^- \rightarrow \bullet OH + HO^- + O_2$ (Eq. 9)

$R/microorganismo + \bullet OH \rightarrow$ Degradation products (Eq. 10)

$R/microorganismo + h_{vb}^+ \rightarrow$ Degradation products (Eq. 11)

Doping TiO_2 with copper has been shown to increase the photocatalytic activity of the material in the presence of visible light by reducing the recombination of charge carriers. Copper oxide, with a narrow Bandgap range (cupric oxide, 1.4 eV; cuprous oxide, 2.2 eV), and a high absorption coefficient, modifies the particle properties, electronic structure, and light absorption of titanium dioxide [11]. These advances are promising for improving the efficiency of water treatment systems and using clean energy [12, 13, 14].

Copper-doped titanium dioxide nanoparticle systems have been widely studied in various photocatalytic applications, such as photocatalytic degradation of dyes [15, 16], photocatalytic water separation [17], antibacterial materials [18, 19, 20] and the photocatalytic reduction of CO_2 [21]. However, the study with emerging contaminants of pharmaceutical origin has been limited.

This research consisted of the synthesis, characterization and evaluation of the photocatalytic activity of copper-doped titanium dioxide nanoparticles, to degrade emerging contaminants of pharmaceutical origin, using artificial solar radiation. The successful demonstration of its effectiveness in the treatment of a common contaminant demonstrates its potential in the conservation and purification of water, becoming an affordable, simple and effective technology.

MATERIALS AND METHODS

Reagent-grade commercial products were used without further purification. Titanium dioxide anatase (TiO_2) 99.5% from Sensient, sodium chloride (NaCl) 100.1% from Fisher Chemical, sodium hydroxide (NaOH) 96% from Erba, copper (II) sulfate pentahydrate ($CuSO_4 \cdot 5H_2O$) 99% from Venesolventes and paracetamol crystalline powder from G. Amphray Laboratories.

Obtaining titanium dioxide nanoparticles (TiO_2 NPs)

Titanium dioxide nanoparticles were obtained by the mechanical grinding method, known as a "top-down" method. The procedure consisted of mixing commercial TiO_2 powder with 5% by weight of NaCl as an inorganic dispersant. The mixture was then added into two plastic containers with ceramic grinding beads and subjected to a continuous grinding process for 4 hours in a Leegol Electric PG-LG-002 ball mill. Once the grinding time was completed, the powder obtained was sieved with a 45 µm sieve, washed three times with distilled water and dried in an oven at 60 °C for 24 hours. Finally, the samples were ground in a mortar and stored in airtight amber containers for later use.

Synthesis of copper-doped titanium dioxide nanoparticles (Cu/TiO_2 NPs)

For the synthesis of Cu/TiO_2 NPs, copper (II) sulfate pentahydrate as a dopant precursor. To do this, 1% by weight of $CuSO_4 \cdot 5H_2O$ was dissolved in 50 mL of distilled water, and then the TiO_2 NPs were added. The mixture was stirred constantly at 50 °C for 2 hours and the pH was adjusted to 8 by adding NaOH solution. Subsequently, drying was carried out at 90 °C for 24 hours, followed by calcination in an oven at 450 °C for 2 hours. The resulting sample was washed to remove any reagent residue and subjected to a second drying at 90 °C. Finally, the sample was crushed in a mortar and stored in an airtight amber container for later use.

Characterization

In this research, dynamic light scattering (DLS) technique was applied to analyze the particle size distribution of both undoped and copper-doped titanium dioxide. The DLS equipment used was developed in the *Laser Spectroscopy*

and Nanotechnology Laboratory of the School of Chemistry of the Faculty of Sciences of the Central University of Venezuela (UCV). Furthermore, scanning electron microscopy (SEM) technique and energy dispersive X-ray spectroscopy (EDS) were used to evaluate the morphology and elemental chemical composition of the synthesized nanoparticles, respectively. For these techniques, a JEOL JSM-6390 SEM equipment was used, equipped with an Oxford Instruments model 7582 x-ray detector.

Topographic analysis of the TiO_2 NPs and Cu/TiO_2 NPs samples was performed using a Bruker Dimension Edge brand atomic force microscope (AFM). X-ray diffraction (XRD) was used with a Bruker D2 PHASER XRD, operating at 30 kV and 10 mA with Cu Kα radiation. The sensor was scanned in an angle range $2\theta = 10° - 70°$, with a step size of 0.02° and a time per step of 1 s. A wavelength of 1.541840 Å and an incidence window of 0.2 mm were used to study the crystalline structure of the materials. Finally, the optical properties of the nanoparticles were characterized by ultraviolet-visible spectroscopy (UV-Vis), adopting the Tauc method to estimate the band gap. These techniques provided accurate and detailed data on the properties of TiO_2 NPs and Cu/TiO_2 NPs.

Photocatalytic evaluation

To evaluate the photocatalytic activity of the previously prepared TiO_2 and Cu/TiO_2 nanoparticles, an acetaminophen solution was used as a model of emerging water contaminant. The concentration of the drug in the solution was 10 ppm, with a pH of 8 to simulate the characteristic acidity of wastewater. The degradation reaction was carried out in a cylindrical borosilicate batch reactor, using natural sunlight. The experiments were carried out on a sunny day until reaching an accumulated energy of 600 KJ/m^2, monitored by a radiometer. The samples were studied with a load of 1.0 g/L under constant stirring. In addition, control tests were performed, including photolysis (without photocatalytic material) and adsorption (in the dark).

During the *in-situ* monitoring of the photocatalytic reaction, the Raman spectroscopy technique was used, which has been widely used in drug quantification studies [22]. The samples were analyzed at room temperature with the objective of quantifying acetaminophen before and after the photocatalytic process. An Eddu Raman TO-ERS-532 system from Thunder Optics was used, equipped with an AvaSpec-Mini spectrometer from Avantes. This spectrometer has a 2048-pixel CMOS detector and a spectral resolution of 0.09 nm. Additionally, the Eddu Raman system includes a 532 nm laser with a line width of 0.1 nm, an optical fiber, a compact Raman probe with a range of up to 175 cm^{-1} for Raman switching, a 20X microscope objective High-quality NA 40 with a working distance of 11.8 mm, a fixed slit of 50 µm and AvaSoft 8 software.

For analysis, a clean and dry liquid sample holder was used, followed by obtaining three spectra for each sample at different positions. This was done to verify the homogeneity of the sample and rule out the presence of photoinduced phenomena. The laser power was 2.8 mW, and the spectra acquisition time was 2 s. Subsequently, the collected data were processed and visualized in the SpectraGryph 1.2 software for further analysis.

RESULTS AND DISCUSSION

DLS characterization

The size of the particles in photocatalytic materials is a crucial factor that influences the optical behavior of the solutions and the efficiency of the photocatalytic process [23]. In this study, dynamic light scattering (DLS) technique was used to characterize the sizes of particle agglomerates in aqueous samples of pure TiO_2, undoped TiO_2 NPs and doped with 1% copper.

Figure 1 shows the hydrodynamic diameters as a function of the distribution. The DLS plots obtained show dashed lines that correspond to the fit with a Beta function. A

hydrodynamic diameter centered at 27 nm, 19 nm and 16 nm was obtained for the commercial TiO_2, the TiO_2 subjected to 4 hours of grinding and the Cu-doped TiO_2, respectively.

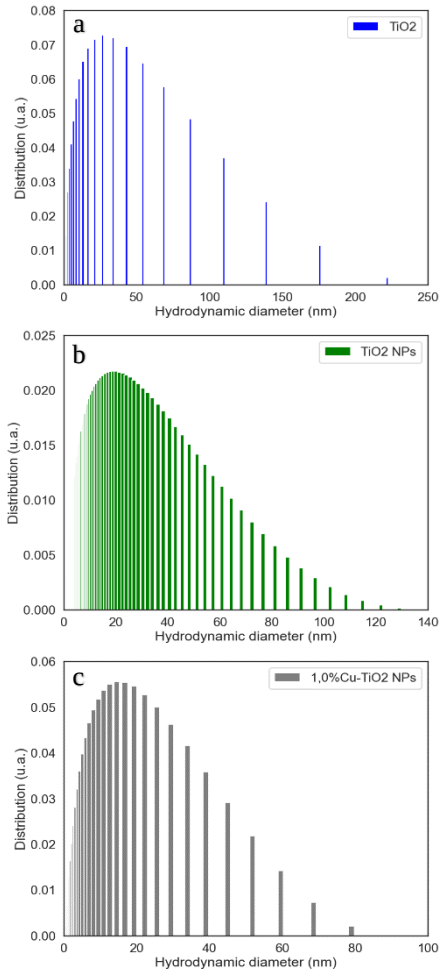

Fig. 1. Particle size distributions of commercial TiO_2 (a), TiO_2 NPs (b) and Cu/TiO_2 NPs (c) measured via DLS.

The DLS technique is a useful tool to determine the effective hydrodynamic diameter, which is a measurement used to describe the apparent size of particles in suspension. This parameter takes into account the behavior of the particles in a liquid medium during the analysis, which provides crucial information about the interaction between the nanoparticles and the solvent [24]. TiO_2 NPs tend to agglomerate when mixed with water, and conventional stirrers cannot break up these hard agglomerates [25]. The doping process in TiO_2 NPs causes significant changes in the dispersive character of the systems and decreases the agglomeration of the particles [26, 27, 28].

The results obtained showed that the copper-doped titanium dioxide samples presented a narrower particle size distribution compared to the undoped TiO_2 samples (Table I). This suggests that the copper doping process caused greater dispersion of the titanium dioxide particles in the solution, resulting in a decrease in particle agglomeration.

Table I. Comparison of hydrodynamic diameters between undoped and 1% Cu doped TiO_2 samples.

Samples	Particle size distribution range (nm)	Average hydrodynamic diameter (D±1) nm
Commercial TiO_2	1 – 225	27
TiO_2 NPs	1 – 130	19
Cu/TiO_2 NPs	1 – 80	16

SEM-EDS characterization

Figure 2 present the scanning electron microscopy (SEM) analysis of TiO_2 NPs. Agglomerates of irregularly shaped, spongy, rough particles and smaller particles were observed on the surface (Figure 2a). In all the samples analyzed, the SEM images reveal three-dimensional structures formed by agglomerates of nanoparticles with a mostly hemispherical morphology. Agglomeration is a natural phenomenon in TiO_2, which tends to form groups of three-dimensional particles [29]. Furthermore, the average size of the particle agglomerates was determined for the TiO_2 NPs, resulting in 190 nm, while in the Cu/TiO_2 NPs it was 171 nm. These results confirm what was previously mentioned in the DLS analysis, where it is evident that the presence of copper reduces the size distribution range of titanium dioxide particle agglomerates.

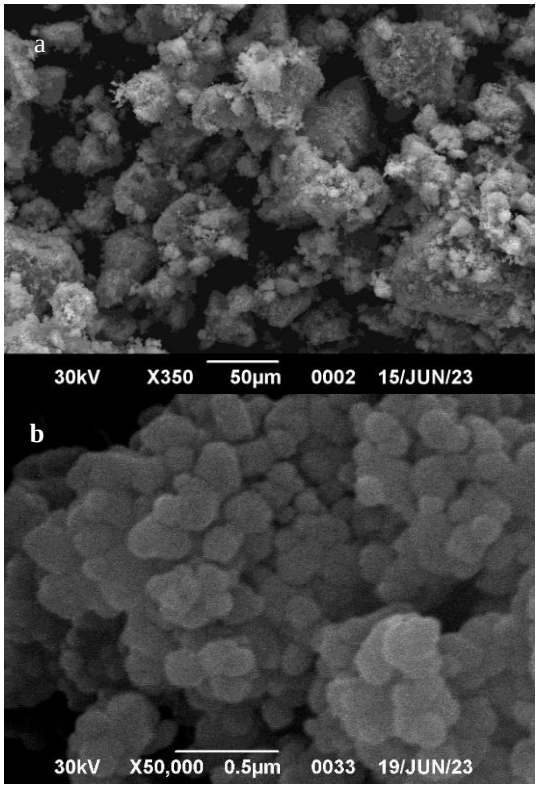

Fig. 2. Micrographs of TiO_2 NPs at different scales: 50 µm (a) and 0.5 µm (b) obtained by SEM.

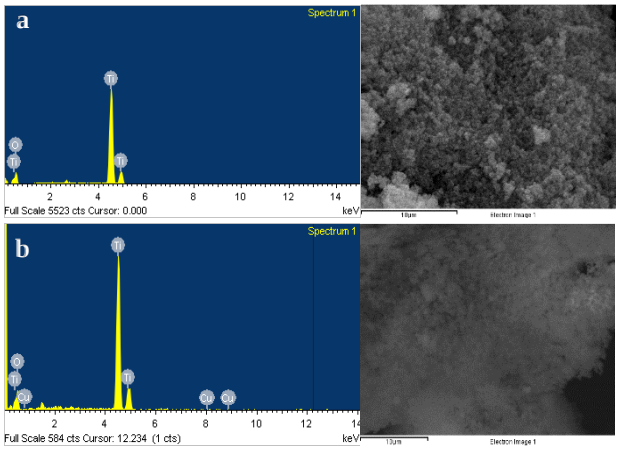

Fig. 3. SEM-EDS analysis of TiO_2 NPs (a) and Cu/TiO_2 NPs (b).

The elemental composition of the titanium dioxide nanoparticles, both undoped and copper-doped, was determined by energy dispersive X-ray spectroscopy (EDS) technique and is presented in fig. 3. According to the EDS analysis, the presence of Ti and O in the TiO_2 NPs, and Ti, O and Cu for the Cu-doped TiO_2 NPs (Table II). The EDX analysis for the undoped TiO_2 NPs is shown in fig. 3a, where the weight percentage of Ti and O was determined to be 52% and 48%, respectively. In both samples, the titanium peak was observed at 0.45, 4.50, and 4.9 keV and the oxygen peak at 0.52 keV. Finally, in the Cu/TiO_2 NPs, the Cu peak was detected at 8.1 keV, 0.94 keV, and 8.9 keV (fig. 3b).

The effectiveness of the impregnation method is demonstrated through the detection of the presence of Cu in the doped TiO_2 NPs, as detailed in Table II. The results obtained are in line with previous studies and confirm the presence of the expected elements in the titanium dioxide nanoparticles after doping with copper [30, 31].

Table II. EDX analysis of undoped and 1% Cu-doped TiO_2 NPs.

Samples	Element	%Weight	%Atomic
TiO_2 NPs	O K	48±4	74±4
	Ti K	52±4	26±4
Cu/TiO_2 NPs	O K	46±4	72±4
	Ti K	52±4	28±4
	Cu K	1.1±0.1	0.42±0.04

AFM characterization

Atomic force microscopy (AFM) analysis of the TiO_2 and Cu/TiO_2 nanoparticles was performed. The samples were observed in tapping mode with a constant of 26 N/m, using a silicon tip on a Bruker Dimension Edge equipment. The AFM technique allowed us to examine the morphology and topography of the nanoparticles obtained in this research.

The results for the TiO_2 NPs are presented in fig. 4, where it is observed that they have a hemispherical morphology (fig. 4a). The AFM topography image with 3D rendering shows a thickness varying between 0.9 nm and 3.8 nm (fig. 4b). In the depth analysis, the maximum point is 20.8 nm (fig. 4c). In addition, the roughness of TiO_2 is presented, where a surface covered by grains of different sizes and shapes, as well as pores and cracks of different dimensions, is evident (fig. 4d). These elements contribute to the surface texture, generating irregularities and roughness on the surface.

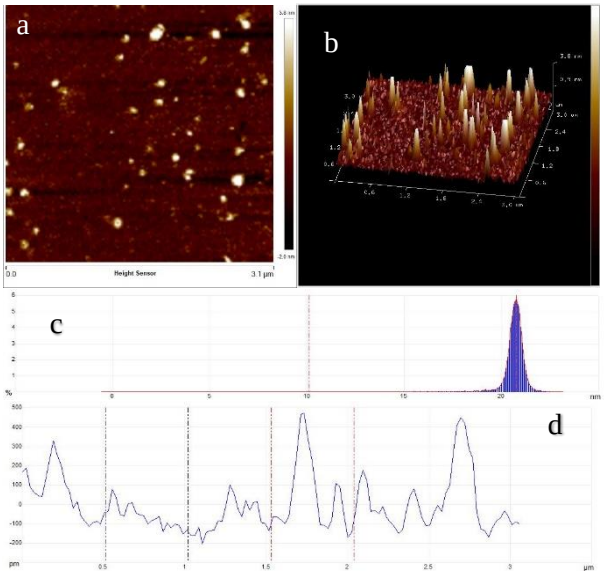

Fig. 4. AFM images of TiO_2 NPs.

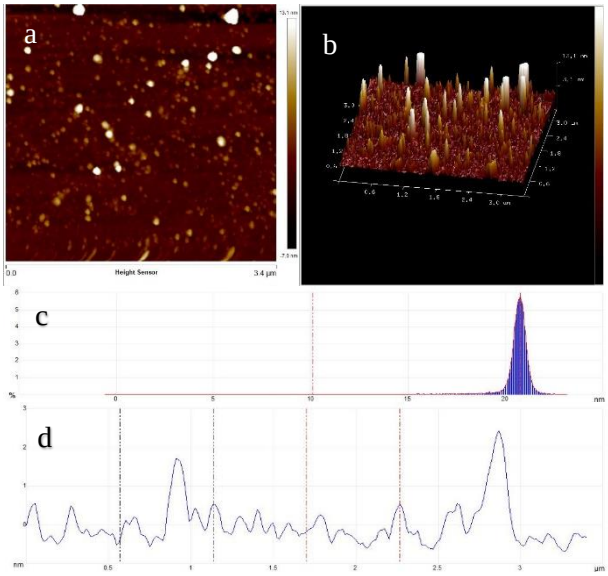

Fig. 5. AFM images of Cu/TiO_2 NPs.

Figure 5 shows the images obtained by AFM for the Cu/TiO2 NPs. In fig. 5a, hemispherical particles are observed, while in fig. 5b a third-dimensional representation of the Cu/TiO_2 NPs is shown, where a thickness ranging between 3.1 nm and 13.1 nm is observed. The depth histogram, plotted in fig. 5c, shows a maximum at 43.6 nm, indicating significant variations in the sample roughness (fig. 5d).

During the analysis of the surface morphology of the particles, the presence of some aggregates and individual particles was observed. The profile indicates that the size of most of the particles is uniform and they have a hemispherical shape in both samples. The AFM image of TiO_2 NPs shows a smoother surface, that is, the surface roughness is lower than that of Cu/TiO_2 NPs. These results coincide with previous research carried out by Pedroza *et al*. (2016) [32], Guerrero (2017) [33] y Raheem *et al*. (2023) [34].

DRX characterization

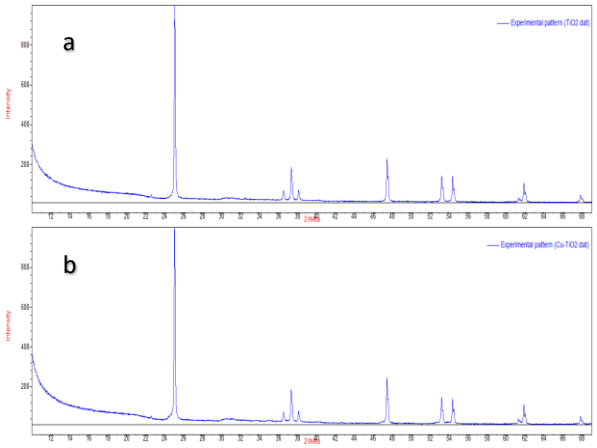

Fig. 6. XRD patterns of TiO_2 NPs (a) and Cu/TiO_2 NPs (b).

The crystallinity and structure of the nanoparticles prepared in this investigation were evaluated by XRD technique. Figure 6a and 6b show the XRD patterns of TiO_2 NPs and Cu/TiO_2 NPs, respectively. The peaks observed at 2θ = 25.10°, 36.56°, 37.40°, 38.16°, 47.48°, 53.22°, 54.38°, 61.90° and 67.88° correspond to the crystal planes of anatase TiO_2 (101), (103), (004), (112), (200), (105), (211), (204) and (116), respectively, coinciding with card number 00-900-8216. There is no evidence of the presence of copper, metal or oxide phases, suggesting that the Cu atoms are in a uniform dispersed state or that the ions successfully entered the TiO_2 crystal lattice. Furthermore, the absence of impurity peaks demonstrates that no additional phases were generated during the Cu-TiO_2 NPs synthesis method used in this investigation. These conclusions are in agreement with previous works by J. C. Lin *et al*. (2018) [35], Preda *et al*. (2022) [36] y Raheem *et al*. (2023) [34].

UV-Vis spectroscopy

The UV-Vis spectroscopy technique was used to analyze the absorbance spectra of TiO_2 NPs and Cu/TiO_2 NPs in a wavelength range of 200 and 900 nm at room temperature. These results are presented in Figs. 7 and 8. From the absorption spectra, the energy gap (E_g) was estimated using the Tauc relationship described in Equation 12.

$$(\alpha h\nu) = A\left(h\nu - E_g\right)^n \quad \text{(Eq. 12)}$$

Here α is the absorption coefficient in cm^{-1}, ν is the frequency of the photon, h is Planck's constant, and $h\nu$ is the energy of the incident photon, A is a constant, n is the exponent that determines the type of transition electronic that causes absorption and could take the values 1/2 or 2 depending on whether the transition is direct or indirect, respectively. The Tauc exponent was estimated directly from experimental UV–vis spectroscopy data [37, 38]. Because optical transitions in TiO_2 are indirect, the value of n was 2. The graph $(\alpha h\nu)^2$ versus $h\nu$ was made and the value of E_g was obtained by extrapolating the linear portion to the photon energy axis.

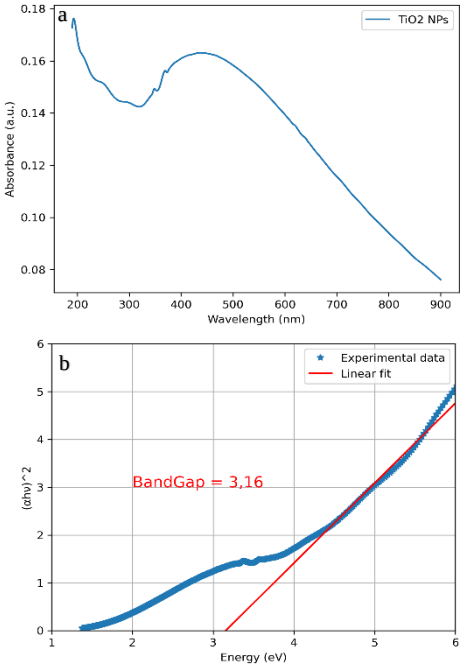

Fig. 7. UV-Vis spectrum of TiO_2 NPs (a) and its Tauc plot (b).

The bandgap value (E_g) of the TiO_2 NPs and Cu/TiO_2 NPs is 3.16 and 2.84, respectively. According to the data summarized in Table III, a decrease of 0.32 eV can be seen in the bandgap of the Cu/TiO_2 NPs compared to the TiO_2 NPs. This reduction in the energy gap can be explained by two factors: (a) quantum confinement phenomena, and (b) the presence of copper oxides that favor the formation of oxygen vacancies and/or the partial reduction of the sites of Ti. The reduction of Ti sites and/or the presence of oxygen vacancies act as a new localized state that contributes to the decrease in bandgap. Therefore, the improvement in light absorption and interfacial charge transfer is expected to be beneficial in increasing the photocatalytic performance of the nanoparticles prepared in this research [39].

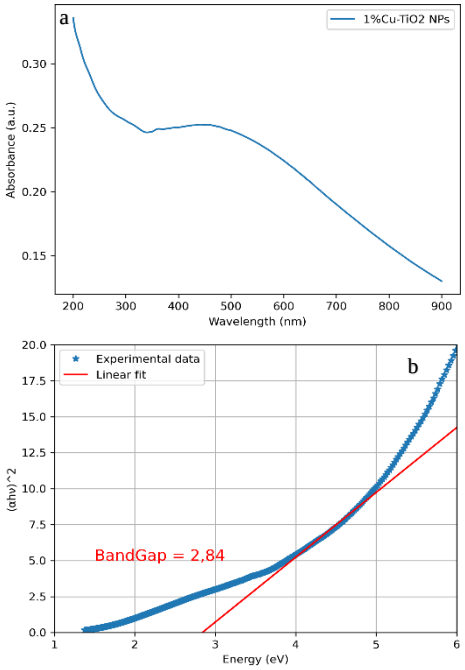

Fig. 8. UV-Vis spectrum of Cu/TiO_2 NPs (a) and its Tauc plot (b).

These results agree with the research of Realpe *et al*. (2017) [40] y Adamu *et al*. (2023) [21], where it is stated that the function of the dopant is to shift the absorption spectrum towards regions of the UV-Vis range. In addition, it is expected that the dopant can act as an electron trap, increasing the photocatalytic efficiency.

Table III. Bandgap and wavelength values for undoped and copper-doped TiO_2 NPs.

Samples	Bandgap (E_g±0,01) eV	Wavelength (λ±1) nm
TiO_2 NPs	3,16	393
Cu/TiO_2 NPs	2,84	437

Photocatalytic activity for the degradation of acetaminophen

Raman spectroscopy is a technique that allows the vibration modes of a sample to be measured, providing detailed information about its chemical composition. The resulting spectrum shows a distribution of peaks corresponding to the specific molecular vibrations of the analyzed sample. These peaks can be used to identify and quantify chemical substances, such as drugs, based on their frequency and intensity [41].

In the specific case of acetaminophen (see fig. 9), its Raman spectrum is dominated by characteristic peaks, such as amide I (C=O) at 1606 cm^{-1}, amide II (C-N stretching, N-H bending) at 1455 cm^{-1}, the C – H bond at 1201 cm^{-1} and the phenyl ring at 800.5 cm^{-1} [22]. These peaks are useful for the identification and quantification of acetaminophen in analyzed samples, whose spectra are shown in fig. 10.

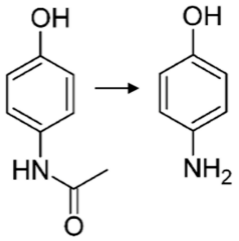

Fig. 9. The chemical structure of acetaminophen and its primary degradation product: p-aminophenol.

Within the framework of this research, the conventional method of measuring Raman peak intensities (area) was used to quantify acetaminophen. It was identified that the most appropriate peak for this purpose is that of amide I (1606 cm^{-1}). A calibration curve was made with acetaminophen solutions in a concentration range of 0.5 ppm to 14 ppm.

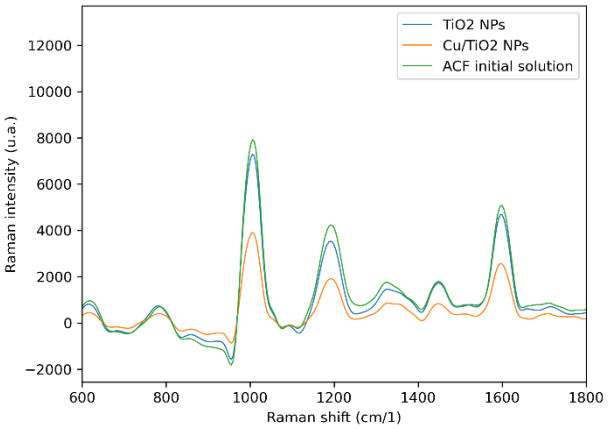

Fig. 10. Raman spectra of acetaminophen in aqueous medium. Initial solution (green), solution photocatalytically treated with TiO_2 NPs (blue) and with Cu/TiO_2 NPs (orange).

The results of drug degradation are detailed in Table IV, where greater degradation of acetaminophen was observed when using doped nanoparticles, suggesting that copper improves the photocatalytic efficiency of titanium dioxide.

Table IV. Values of percentage of photocatalytic degradation of acetaminophen (ACP).

Samples	% degradation of ACP
TiO_2 NPs	38,5
Cu/TiO_2 NPs	77,4

These results can be explained by considering that the inclusion of an electron trap minimizes the unwanted recombination of charge carriers. The selection of metal ions with a positive reduction potential compared to TiO_2 is ideal as an electron trap. Given the standard redox potential of Cu ions in equations (13), (14) and (15), these are excellent for minimizing charge carrier recombination [21]:

$$Cu^{2+} + e^- \rightarrow Cu^+, E^\circ = 0{,}17\,V \quad \text{(Eq. 13)}$$

$$Cu^{2+} + 2e^- \rightarrow Cu^0, E^\circ = 0{,}34\,V \quad \text{(Eq. 14)}$$

$$Cu^+ + e^- \rightarrow Cu^0, E^\circ = 0{,}52\,V \quad \text{(Eq. 15)}$$

In summary, the addition of Cu as a dopant generates a level of Cu^{2+} impurity below the conduction band of TiO_2. During light irradiation, the electron in the valence band can be excited toward the Cu^{2+} trap level, forming electron-hole pairs with the same number of positively charged holes. This proximity facilitates the release of the electron trapped in Cu^{2+} and its transfer to a neighboring surface Ti^{4+}, which decreases the recombination rate of the electron-hole pair and prolongs the lifetime of the charge carriers. Furthermore, Cu^{2+} doping in the TiO_2 lattice generates oxygen vacancies to maintain charge neutrality, inducing visible light absorption [16].

CONCLUSIONS

In this study, the preparation of titanium dioxide nanoparticles doped with 1% copper was carried out by wet impregnation method. The prepared samples had an average hydrodynamic diameter of 16±1 nm, with relatively rough surfaces and a hemispherical morphology. It was observed that copper-doped TiO_2 NPs exhibited enhanced photocatalytic activity compared to undoped nanoparticles, when exposed to natural sunlight irradiation. The copper-doped TiO_2 structure was able to effectively broaden its absorption capacity in the visible spectrum of sunlight (400-700 nm), as copper induced some doping states near the top of the valence band, thus enhacing the visible absorption through the Cu 3*d*-Ti 3*d* optical transition.

These results suggest that TiO_2 NPs doped with 1% copper could be used to promote the photodegradation of acetaminophen under visible light irradiation, as well as for the treatment of water contaminated with organic compounds.

ACKNOWLEDGEMENT

The authors would like to thank the National Fund for Science and Technology for the financial support granted for the development of this research project.

CONFLICT OF INTERESTS

The authors declare that they have no conflict of interests.

REFERENCES

[1] Naciones Unidas, “Objetivo 6. Agua Limpia Y Saneamiento: Por Que Es Importante,” *Sustainable development goals*. pp. 1–2, 2015. [Online]. Available: shorturl.at/cdry4

[2] D. Pino, “Determinación de fármacos en agua residual hospitalaria y aplicación del proceso de fotocatálisis heterogénea solar para su degradación,” Universidad Autónoma de Nuevo León, 2018.

[3] R. NORMAN, “Base de datos de sustancias NORMAN,” *Paracetamol*, 2023. https://www.norman-network.com/nds/susdat/susdatSearchShow.php

[4] K. Poddar, D. Sarkar, D. Chakraborty, P. Patil, S. Maity, and A. Sarkar, “Paracetamol biodegradation by Pseudomonas strain PrS10 isolated from pharmaceutical effluents,” *Int. Biodeterior. Biodegradation*, vol. 175, p. 105490, Nov. 2022, doi: 10.1016/j.ibiod.2022.105490.

[5] A. Al-Kaf, N. Khalid, Q. Yusuf, and W. Edrees, “Occurrence of Paracetamol in Aquatic Environments and Transformation by Microorganisms: A Review Methicillin-resistant Staphylococcus aureus View project Isolation and Identification of a New Fungal Species Degrading Paracetamol Isolated from Yemeni Envir,” *Chronicles Pharm. Sci.*, vol. 1.6, no. December, pp. 341–355, 2017, [Online]. Available: https://www.researchgate.net/publication/322041109

[6] E. Serna *et al.*, “Degradation of seventeen contaminants of emerging concern in municipal wastewater effluents by sonochemical advanced oxidation processes,” *Water Res.*, vol. 154, pp. 349–360, May 2019, doi:

10.1016/j.watres.2019.01.045.

[7] R. Tenorio, "Degradación fotocatalítica de fármacos de un efluente hospitalario: identificación de los intermediarios y subproductos de reacción," Universidad Autónoma de Nuevo León, 2020.

[8] M. Ouzzine, "Nanoparticulas de TiO_2 para la oxidación fotocatalítica de propeno en fase gas a baja concentración," Universidad de Alicante, 2014. [Online]. Available: www.eltallerdigital.com

[9] A. Fujishima and K. Honda, "Electrochemical Photolysis of Water at a Semiconductor Electrode," *Nature*, vol. 238, pp. 37–38, 1972.

[10] L. Espiga, "Materiales fotocatalíticos y sus aplicaciones en construcción," Universidad Politécnica de Catalunya, 2018. [Online]. Available: https://www.redalyc.org/pdf/115/11502906.pdf

[11] M. Sahu and P. Biswas, "Single-step processing of copper-doped titania nanomaterials in a flame aerosol reactor," *Nanoscale Res. Lett.*, vol. 6, no. 1, p. 441, Jul. 2011, doi: 10.1186/1556-276X-6-441.

[12] M. Rodríguez and C. Barrera, *Procesos de oxidación avanzada en el tratamiento de agua*, Primera ed., vol. 1. Toluca: Universidad Autónoma del Estado de México, 2020. [Online]. Available: http: //www.uaemex.mx

[13] M. Nevárez, P. Espinoza, F. Quiroz, and B. Ohtani, "Fotocatálisis: inicio, actualidad y perspectivas a través del TiO2," *Av. en Química*, vol. 12, pp. 45–59, 2017.

[14] R. Kaur *et al.*, "Cu-BTC metal organic framework (MOF) derived Cu-doped TiO_2 nanoparticles and their use as visible light active photocatalyst for the decomposition of ofloxacin (OFX) antibiotic and antibacterial activity," *Adv. Powder Technol.*, vol. 32, no. 5, pp. 1350–1361, May 2021, doi: 10.1016/j.apt.2021.02.037.

[15] X. Zhu *et al.*, "One-step hydrothermal synthesis and characterization of Cu-doped TiO_2 nanoparticles/nanobucks/nanorods with enhanced photocatalytic performance under simulated solar light," *J. Mater. Sci. Mater. Electron.*, vol. 30, no. 14, pp. 13826–13834, 2019, doi: 10.1007/s10854-019-01766-3.

[16] H. Liu, M. Zou, B. Viliam Hakala, R. Sefiu Abolaji, and M. Yang, "Synthesis, characterization of Cu, N co-doped TiO_2 microspheres with enhanced photocatalytic activities," *Adv. Mater. Sci.*, vol. 2, no. 1, pp. 1–7, 2017, doi: 10.15761/AMS.1000114.

[17] C. Cheng, W.-H. Fang, R. Long, and O. Prezhdo, "Water Splitting with a Single-Atom Cu/TiO_2 Photocatalyst: Atomistic Origin of High Efficiency and Proposed Enhancement by Spin Selection," *JACS Au*, vol. 1, no. 5, pp. 550–559, May 2021, doi: 10.1021/jacsau.1c00004.

[18] X. Zheng, Z. Shen, C. Cheng, L. Shi, R. Cheng, and D. Yuan, "Photocatalytic disinfection performance in virus and virus/bacteria system by $Cu\text{-}TiO_2$ nanofibers under visible light," *Environ. Pollut.*, vol. 237, pp. 452–459, 2018, doi: 10.1016/j.envpol.2018.02.074.

[19] S. Mathew *et al.*, "Cu-Doped TiO_2: Visible light assisted photocatalytic antimicrobial activity," *Appl. Sci. MDPI*, vol. 8, no. 11, 2018, doi: 10.3390/app8112067.

[20] R. Bucuresteanu *et al.*, "Preliminary Study on Light-Activated Antimicrobial Agents as Photocatalytic Method for Protection of Surfaces with Increased Risk of Infections," *Mater. MDPI*, vol. 14, no. 5707, 2021, doi: 10.3390/ma14185307.

[21] A. Adamu, M. Isaacs, K. Boodhoo, and F. R. Abegão, "Investigation of Cu/TiO_2 synthesis methods and conditions for CO_2 photocatalytic reduction via conversion of bicarbonate/carbonate

to formate," *J. CO_2 Util.*, vol. 70, no. January, p. 102428, Apr. 2023, doi: 10.1016/j.jcou.2023.102428.

[22] V. Borio, R. Vinha, R. Nicolau, H. De Oliveira, C. De Lima, and L. Silveira, "Quantitative Evaluation of Acetaminophen in Oral Solutions by Dispersive Raman Spectroscopy for Quality Control," *Spectrosc. An Int. J.*, vol. 27, no. 4, pp. 215–228, 2012, doi: 10.1155/2012/108041.

[23] A. Cassano and O. Alfano, "Reaction engineering of suspended solid heterogeneous photocatalytic reactors," *Catal. Today*, vol. 58, no. 2–3, pp. 167–197, May 2000, doi: 10.1016/S0920-5861(00)00251-0.

[24] E. Mosquera, N. Rosas, A. Debut, and V. Guerrero, "Sintesis y caracterizacion de nanoparticulas de Dioxido de Titanio obtenidas por el metodo sol-gel," *Rev. Politécnica*, vol. 36, no. 3, p. 7, 2015, [Online]. Available: https://www.revistapolitecnica.epn.edu.ec/ojs2/index.php/revista_politecnica2/article/view/525/pdf

[25] D. Shafaei, S. Yang, L. Berlouis, and J. Minto, "Multiscale pore structure analysis of nano titanium dioxide cement mortar composite," *Mater. Today Commun.*, vol. 22, no. August 2019, p. 100779, Mar. 2020, doi: 10.1016/j.mtcomm.2019.100779.

[26] M. Sahu, K. Suttiponparnit, S. Suvachittanont, T. Charinpanitkul, and P. Biswas, "Characterization of doped TiO_2 nanoparticle dispersions," *Chem. Eng. Sci.*, vol. 66, no. 15, pp. 3482–3490, Aug. 2011, doi: 10.1016/j.ces.2011.04.003.

[27] K. Siwinska, D. Paukszta, A. Piasecki, and T. Jesionowski, "Synthesis and physicochemical characteristics of titanium dioxide doped with selected metals," *Physicochem. Probl. Miner. Process.*, vol. 50, no. 1, pp. 265–276, 2014, doi: 10.5277/ppmp140122.

[28] R. Li, T. Li, and Q. Zhou, "Impact of Titanium Dioxide (TiO2) Modification on Its Application to Pollution Treatment—A Review," *Catalysts*, vol. 10, no. 7, p. 804, Jul. 2020, doi: 10.3390/catal10070804.

[29] P. Monchot *et al.*, "Deep Learning Based Instance Segmentation of Titanium Dioxide Particles in the Form of Agglomerates in Scanning Electron Microscopy," *Nanomaterials*, vol. 11, no. 4, p. 968, Apr. 2021, doi: 10.3390/nano11040968.

[30] L. Clarizia *et al.*, "Effect of surface properties of copper-modified commercial titanium dioxide photocatalysts on hydrogen production through photoreforming of alcohols," *Int. J. Hydrogen Energy*, vol. 42, no. 47, pp. 28349–28362, Nov. 2017, doi: 10.1016/j.ijhydene.2017.09.093.

[31] Y. P. Lim and Y. C. Lim, "Synthesis of Hybrid Cu-Doped TiO_2 Photocatalyst for Dye Removal," *Key Eng. Mater.*, vol. 797, pp. 84–91, Mar. 2019, doi: 10.4028/www.scientific.net/KEM.797.84.

[32] G. Pedroza, "Evaluación de la actividad fotocatalítica y toxicológica de materiales nanoestructurados de dióxido de titanio dopado con cobre," Universidad Autonoma de Aguascalientes, 2016.

[33] S. Guerrero, "Síntesis y caracterización de materiales base óxido de zinc-óxido de cobre /dióxido de titanio," Instituto Politécnico Nacional de México, 2017.

[34] S. Raheem, J. Sattar, and S. Al-Jubori, "Characterization of Titanium dioxide (TiO_2) Nanoparticles Biosynthesized using Leuconostoc spp. Isolated from Cow's Raw Milk," *Proc. Pakistan Acad. Sci. B. Life Environ. Sci.*, vol. 60, no. 1, pp. 133–142, Mar. 2023, doi: 10.53560/PPASB(60-1)823.

[35] J. C. Lin, K. Sopajaree, T. Jitjanesuwan, and M. Lu, "Application of visible light on copper-doped titanium dioxide catalyzing degradation of chlorophenols," *Sep. Purif. Technol.*, vol. 191, no.

June 2017, pp. 233–243, Jan. 2018, doi: 10.1016/j.seppur.2017.09.027.

[36] S. Preda *et al.*, "Photocatalytic and Antibacterial Properties of Doped TiO_2 Nanopowders Synthesized by Sol−Gel Method," *Gels*, vol. 8, no. 10, p. 673, Oct. 2022, doi: 10.3390/gels8100673.

[37] H. Łukasz, O. Adrian, G. Katarzyna, and S. Katarzyna, "A facile method for Tauc exponent and corresponding electronic transitions determination in semiconductors directly from UV–Vis spectroscopy data," *Opt. Mater. (Amst).*, vol. 127, p. 112205, 2022, doi: https://doi.org/10.1016/j.optmat.2022.112205Obt .

[38] Ł. Haryński, A. Olejnik, K. Grochowska, and K. Siuzdak, "A facile method for Tauc exponent and corresponding electronic transitions determination in semiconductors directly from UV–Vis spectroscopy data," *Opt. Mater. (Amst).*, vol. 127, no. April, p. 112205, May 2022, doi: 10.1016/j.optmat.2022.112205.

[39] H. Hamad *et al.*, "The superior photocatalytic performance and DFT insights of S-scheme $CuO@TiO_2$ heterojunction composites for simultaneous degradation of organics," *Sci. Rep.*, vol. 12, no. 1, p. 2217, Feb. 2022, doi: 10.1038/s41598-022-05981-7.

[40] Á. Realpe, D. Núñez, and M. Acevedo, "Effect of Cu on optical properties of TiO_2 nanoparticles," *Contemp. Eng. Sci.*, vol. 10, no. 31, pp. 1539–1549, 2017, doi: 10.12988/ces.2017.711182.

[41] C. Shende, W. Smith, C. Brouillette, and S. Farquharson, "Drug Stability Analysis by Raman Spectroscopy," *Pharmaceutics*, vol. 6, no. 4, pp. 651–662, Dec. 2014, doi: 10.3390/pharmaceutics6040651.